

# NANOSENSORS ENGINEERING:

## II. SUPERFICIAL FUNCTIONALIZATION OF SnO<sub>2</sub> NANOWIRE FOR SENSING PERFORMANCE IMPROVEMENT

Serghei Dmitriev

Physics Department, Moldova State University  
60, A. Mateevici str., Chisinau, MD-2009, Moldova

E-mail: [sdmitriev@usm.md](mailto:sdmitriev@usm.md)

*Abstract - Paper presents results of study aimed the tin dioxide nanowire gas sensing performance improvement via in situ functionalization with NiO. Developed nanostructures have demonstrated improved by order gas sensitivity toward H<sub>2</sub> and CO and drastic increase of selectivity to H<sub>2</sub> against CO. Obtained results are discussed from the point of view of NiO/SnO<sub>2</sub> heterojunction formation and its influence on electrical transport through nanowire and nanowire interaction with target gases.*

**Key words:** Nanowire, tin dioxide, nickel oxide, chemoresistor, functionalization, heterojunction

### I. INTRODUCTION

Chemical nanosensors represent high interest for researchers and manufacturers in the field of gas sensorics due to their potential to detect very low concentrations of active impurities in atmosphere [1-5]. Capability to detect low concentrations of target gases is connected usually with extremely high surface-to-volume ratio of given nanostructures as their electrical characteristics are highly sensitive to surface-adsorbed gaseous species. However, the problem of selectivity of low-dimensional gas sensitive structures remains and on the nanoscopic level. There are known some attempts to improve gas sensing performance through the electron density manipulation in the nanodimensional structures (NDS) using UV irradiation [6] or nanowire configured as field effect transistor (FET) [7]. The attempt to functionalize polysilicon mesowire using Pd is well described in [8], however, for H<sub>2</sub> sensor there was used multi-step

micromachining process. At that Pd was deposited along of all top side of polysilicon nanowire, forming practically continuous thin film on the NW surface. The resulting nanodevice was metal/semiconductor Schottky diode. Another approach was demonstrated in [9], where Pd was deposited already as particles on the surface of SnO<sub>2</sub> NW.

Here we report an approach to SnO<sub>2</sub> nanowire gas sensing performance improvement based on *in situ* nanowire surface functionalization with NiO<sub>x</sub> clusters. In essence, the task is to format the multitude nanodimensional p-n heterojunctions on the surface of such nanostructure as nanowire. Nickel oxide, in its non-stoichiometric NiO<sub>x</sub> form, in contrast to metallic palladium, is semiconducting material of p-type conductivity. It is intriguing from the physical point of view material due to its useful catalytic [10-12], magnetic [13], optical [14] and electrochromic properties [15]. In less degree, nickel oxide is known as gas sensing material [16-20].

As to SnO<sub>2</sub> it is well known and wide used n-type semiconducting gas sensitive material with wide band-gap (3.6 eV) with the rutile structure [21]. Electrical conductivity in tin oxide is result of non-stoichiometry stipulated basically by point atomic defects (oxygen vacancies). Single and double charged oxygen vacancies form two levels in forbidden zone - 30 meV and 150 meV correspondingly - below conductance band [22]. Additional levels arise at the chemisorption of gaseous molecules on the surface of semiconductor that leads to the space charge region alteration and band bending changing. These phenomena are accompanied with conductivity modulation. Deposition of the p-type NiO<sub>x</sub> clusters on the surface of SnO<sub>2</sub> NW can dramatically change the character of NW interaction with gases due to the formation of multitude local NiO(*p*)-SnO<sub>2</sub>(*n*) heterojunctions on NW surface.

## II. EXPERIMENTAL AND METHODS

### a) General

Rutile structured SnO<sub>2</sub> had been obtained as nanowire on Si/SiO<sub>2</sub> substrate through the standard vapor-solid procedure [23] at temperature T=900°C from SnO powder as precursor. Argon gas of research purity was used as carrier gas in the tin dioxide nanowire grown process.

X-ray diffraction (XRD) study and Scanning Electron Microscopy (SEM) were used to characterize the structure, composition and shape of the SnO<sub>2</sub> NWs.

Successive Ti/Au (20/500 nm) PVD deposition through the shadow mask in high vacuum was used to produce electrical contacts to individual NWs. As fabricated SnO<sub>2</sub> nanowire based chemoresistor was mounted in UHV chamber with electrical feed-through and gas delivering system governed by the computer.

Chemoresistor's electrical characteristics (I-V curves) were measured in two-point configuration under vacuum conditions. Gas sensing response toward inflammable (H<sub>2</sub>) (P<sub>H<sub>2</sub></sub>=3x10<sup>-4</sup> Torr) and toxic (CO) (P<sub>CO</sub>=3x10<sup>-4</sup> Torr) gases was measured with oxygen background (P<sub>O<sub>2</sub></sub>=1x10<sup>-4</sup> Torr). The chemoresistor was kept at T=350°C for all electrical and gas sensing measurements.

### **b) SnO<sub>2</sub> nanowire functionalization**

Before exposing chemoresistor to Ni flux the system was pumped to vacuum conditions P=1x10<sup>-6</sup> Torr and nanowire was exposed to UV light for 30 minutes for NW surface cleaning of residue gases. Functionalization process was performed under the 6x10<sup>-6</sup> Torr vacuum conditions through standard PVD process. Sample's temperature was kept at that at T=350°C. Ni deposition process was controlled through the chemoresistor conductance change monitoring by computer.

For the process of *in situ* functionalization with NiO<sub>x</sub> there was used the *deposition - electrical - gas sensitive measurement cycle*. Deposition time for NiO<sub>x</sub> was determined from preliminary experiments, and has amounted 500 seconds per deposition. The deposition process itself was repeated four times and it has been traced via controlling the NW current changing. After deposition had ceased nanowire was subjected to pulses of H<sub>2</sub> (P<sub>H<sub>2</sub></sub>=3x10<sup>-4</sup> Torr) (inflammable gas) and CO (P<sub>CO</sub>=5x10<sup>-5</sup> Torr) (toxic gas) with O<sub>2</sub> background (P<sub>O<sub>2</sub></sub>=1x10<sup>-4</sup> Torr).

Considering the SnO<sub>2</sub> functionalization with NiO<sub>x</sub> we should note that for its deposition there was used metal Ni. At that we took into account that fact that Ni can be oxidized at sufficiently low temperature even in the vacuum condition interacting with residual oxygen (P=6x10<sup>-6</sup> Torr). Briefly, we supposed that in our case the Ni deposited on the NW surface will transform into the NiO<sub>x</sub>. We say NiO<sub>x</sub> because in reality the oxidation of Ni is not complete even at atmospheric pressure and huge amount of oxygen vacancies is presented in the material, providing its semiconducting properties (pure NiO is isolator). To verify this idea we deposited Ni between another two pads (which were under the small voltage) to form a film. We had been continued deposition process before current between these two pads has appeared. If as-grown film is really

NiO<sub>x</sub> but not metallic Ni film it should demonstrate the behavior in gaseous atmosphere characteristic for *p*-type materials, i.e. current through it should increase at the leaking-in of oxidizing gas. The last was observed at the chamber feeding with oxygen (Figure 1) of  $P=1 \times 10^{-4}$  Torr, testifying the formation of NiO<sub>x</sub> but not pure Ni clusters on the surface of SnO<sub>2</sub> nanowire.

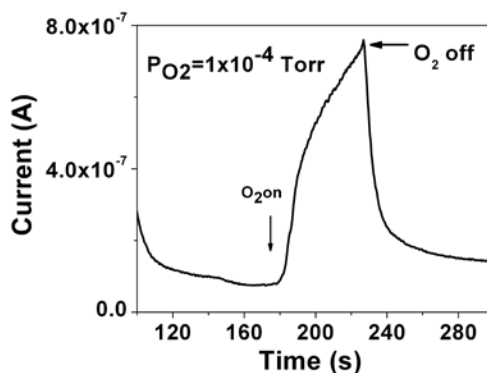


Figure 1. NiO<sub>x</sub> film response toward oxygen ( $P_{O_2}=1 \times 10^{-4}$  Torr)

So, further, we will speak about SnO<sub>2</sub> functionalization with NiO<sub>x</sub> clusters, role of which in the tin oxide nanowire response to different active gases will be discussed below.

### III. RESULTS AND DISCUSSION

#### a) The as-fabricated SnO<sub>2</sub> nanowire

Presented in Figure 2 X-ray diffraction pattern confirms that fabricated nanostructure possesses high level of crystallinity and it can be indexed on the basis of the rutile cell:  $a=0.4760$

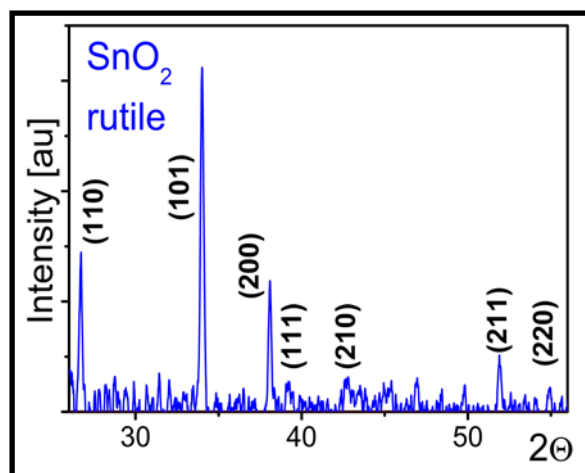


Figure 2. XRD spectra of SnO<sub>2</sub> nanowire.

nm and  $c=0.3178$  nm [24]. There are some major peaks, which can be ascribed to (110), (101), (200), (211) crystal planes correspondingly, characteristic for tetragonal structure of the SnO<sub>2</sub>.

The morphology of as-grown SnO<sub>2</sub> NWs (with already deposited Ti/Au electrodes) was characterized through scanning electron microscopy (SEM), results of which are presented in Figure 3. Grown NWs have had an average diameter about 80 nanometers and their length have amounted approximately 15 microns.

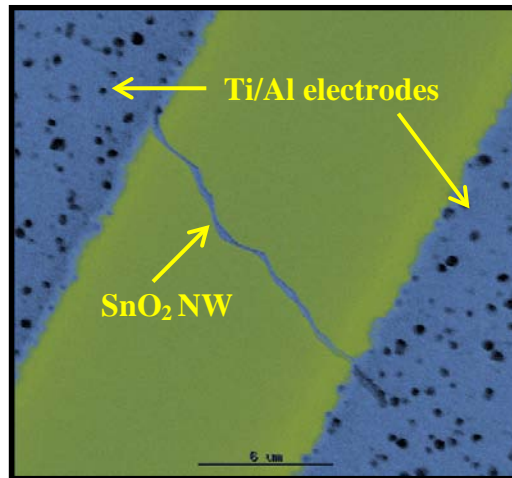


Figure 3. SEM image of SnO<sub>2</sub> NW based nanostructure.

Preliminary testing has shown that chemoresistors demonstrate typical for *n*-type materials electrical behavior, i.e. its conductance decreases in the presence of oxidizing gases (O<sub>2</sub>) and increases in the presence of reducing gases such as H<sub>2</sub>, CO, etc.

### b) Electrical and gas sensitive properties

In Figure 4 one can see the representative I-V curves measured before and after already the first process on NiO<sub>x</sub> deposition on the SnO<sub>2</sub> nanowire surface (under vacuum conditions). One can see that functionalization leads to the significant (more than one order) decrease of the current through nanowire. In particular, the values of current at the voltage  $U=6$  Volts have amounted  $1.84 \times 10^{-6}$  amperes before deposition and  $1.16 \times 10^{-7}$  amperes after the process correspondingly (ratio of the currents at that is equal to 15.86. One can see also that recorded I-V characteristics keep their linearity and after NiO deposition process. The origin of such drastic decrease in conductivity will be discussed along with the results on gas sensing performance.

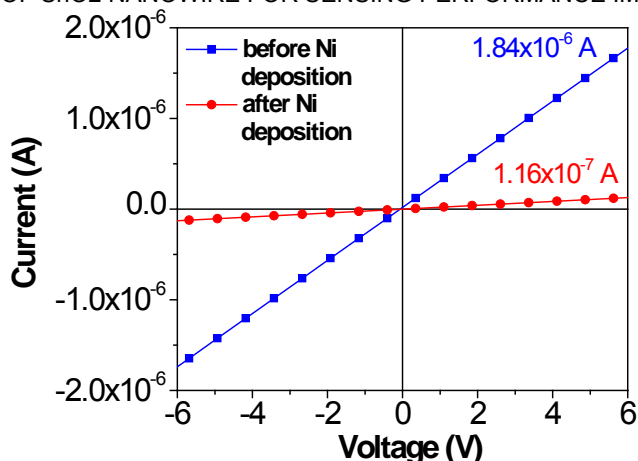


Figure 4. I-V characteristics of SnO<sub>2</sub> NW before and after the first process on Ni deposition.

Typical responses of the functionalized with NiO<sub>x</sub> chemoresistors are shown in Figure 5. Determined from the graph response times (time of achievement of 80% of the current maximum) have amounted 30 s for hydrogen and 80 s for CO.

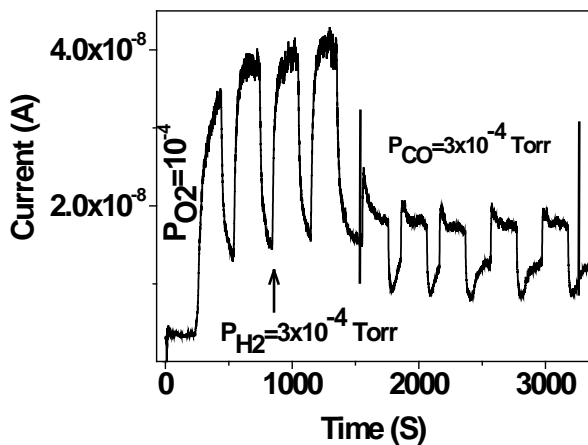


Figure 5. Typical response of NiO<sub>x</sub> functionalized SnO<sub>2</sub> NW toward H<sub>2</sub> and CO gases.

On the basis of these data the sensitivities of nanodevices to both gases on dependence on the amount of deposition processes were calculated as value  $S = G_{gas}/G_{O_2}$  where  $G_{O_2}$  is NW electrical conductivity in oxygen background and  $G_R$  is its conductivity in the presence of target gas (Figure 6). One can see that we have the sensitivity growth with maximum to both gases after third deposition and  $S$  is almost twice decreasing after the fourth deposition process.

Observed behavior we connect with the transformation of numerous and separated NiO clusters on SnO<sub>2</sub> NW surface in the regions of nanodimensional continuous film which:

- 1) are shunting the current through SnO<sub>2</sub> NW due to the percolation effects and
- 2) are decreasing the SnO<sub>2</sub> NW surface area open for interaction with gaseous species in air.

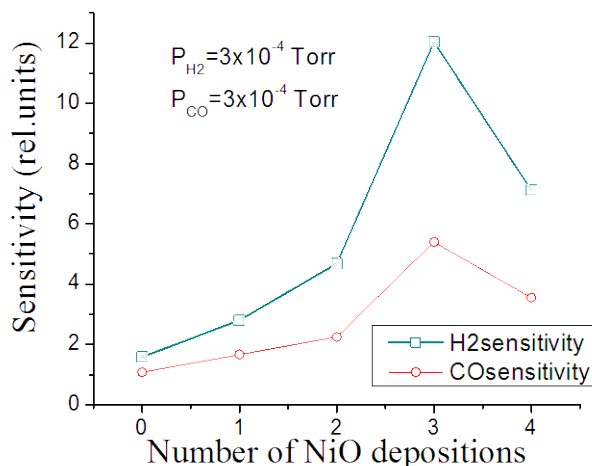


Figure 6. Sensitivities of NiO functionalized SnO<sub>2</sub> NW as function of the number of depositions.

Another feature of the obtained data is connected with interaction of functionalized SnO<sub>2</sub> NW with CO gas. In the case of NiO<sub>x</sub> functionalization sensitivity to CO ( $S_{CO}$ ) repeats the shape of sensitivity to H<sub>2</sub> ( $S_{H_2}$ ) although is lower.

### c) Electrical and gas sensing performance results analysis

Starting discussion of obtained results, we should note that at least three processes *can* take place on the surface of SnO<sub>2</sub> nanowire at the functionalization with NiO<sub>x</sub>:

- 1) Ni atoms interaction with SnO<sub>2</sub> NW matrix and their incorporation in it;
- 2) Superficial Ni interaction with residual oxygen in the vacuum chamber and following oxidation to NiO<sub>x</sub>;
- 3) NiO molecules/NiO<sub>x</sub> particles coalescence to the NiO<sub>x</sub> clusters on the SnO<sub>2</sub> NW surface.

As to the first process, the positioning of the Ni atoms - on the surface or in the bulk of oxide material - it remains still under the question. As the value of Ni<sup>2+</sup> ionic radius (0.70 Å) is very close to that of Sn<sup>4+</sup> (0.69 Å), it was suggested that Ni atoms are most likely to be located in the

positions of Sn atoms in the metal oxide matrix and so the solubility of nickel in the bulk of SnO<sub>2</sub> crystallites is very high [25]. Such substitution will create impurity acceptor Ni<sub>Sn</sub><sup>2+</sup> centers and will compensate the intrinsic donor type oxygen vacancies centers in the SnO<sub>2</sub> surface and subsurface region leading to the conductivity decrease. However, as functionalization process was carried out at T=350°C we do not expect any strong diffusion of Ni atoms inside of the tin dioxide bulk. Besides that the recent studies [20] have presented the evidence of Ni segregation onto the SnO<sub>2</sub> surface. Given segregation phenomenon of Ni onto the tin dioxide surface was confirmed by means of very different techniques (XRD, DRIFT, EDS and HRTEM). That allows us to suggesting that if even some Ni atoms could diffuse in the SnO<sub>2</sub> bulk in the reality they play a very restricted role in conductance mechanism changing. So, further we will proceed in our discussion from the idea that Ni particles are concentrating basically on the surface of NW.

Further consequent Ni deposition leads, in our opinion, to the local Ni islands coalescence into the larger continuous clusters. Simultaneously, the oxidation of Ni particles to the NiO<sub>x</sub> is occurring in accordance with equations [26]:



Equation (1) describes the interaction of the oxygen dissociatively chemisorbed on the surface with Ni particles but equation (2), in its turn, describes the process of slow diffusion of oxygen inside the cluster (into a subsurface layer) and Ni oxidation to NiO<sub>x</sub> form in a consecutive step.

The experiments on oxidation of 50 nm Ni film in vacuum have shown that such oxidation process is already observed at T=473K (200°C) [27]. In our case all experiments are performed at the T=350°C under vacuum 10<sup>-6</sup> Torr that allows us to consider that oxidation of Ni particles or clusters to NiO<sub>x</sub> should take place. Since NiO<sub>x</sub> is *p*-type semiconductor the formation of multitude local NiO(*p*)-SnO<sub>2</sub>(*n*) heterojunctions should take place on the surface of nanowire. Model of such type chemoresistor is presented in Figure 7.

The last one leads to the depletion regions formation and conductance channel narrowing/modulation and, as result, nanowire resistance and gas sensitivity growth. The deepness of conductance modulation will depend strongly on the amounts and sizes of such *p-n* junctions.

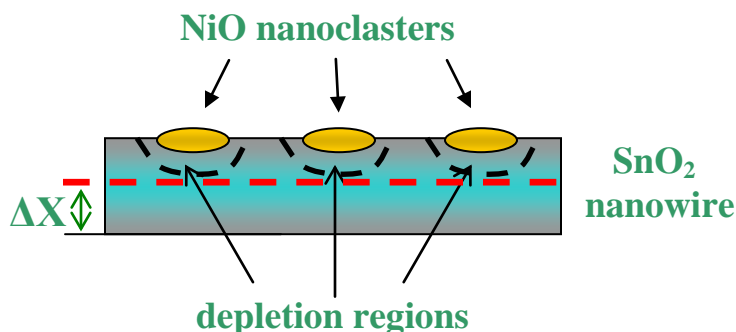


Figure 7. Model of the NiO(*p*)-SnO<sub>2</sub>(*n*) heterojunction type chemoresistor

Considering the NiO<sub>x</sub> clusters influence on sensitivities to the both gases we can see that changes of the  $S_{H_2}$  are more pronounced than in comparison with  $S_{CO}$  as amount of depositions grows. Such definite selectivity can be understood if to consider the reaction of NiO surface with gaseous molecules of CO [28]:



where (s) and (g) mean *solid* and *gas* states correspondingly. It was shown that in given reaction, yielding Ni atoms and CO<sub>2</sub>, there is a barrier of 15 kcal/mol relative to the reactants, occurring at the second reaction step. Proceeding from that, nickel oxide material is expected to be less efficient for oxidizing CO to CO<sub>2</sub> [28]. Nickel oxide can also form the CONiO complex but the latter would rather dissociate back to NiO + CO, requiring about 10 kcal/mol than to produce Ni + CO<sub>2</sub> via the barrier of 25 kcal/mol. So, as result, the sensitivity of SnO<sub>2</sub> NW functionalized with NiO to CO gas is not so high in comparison with hydrogen.

As to sensitivity and selectivity to H<sub>2</sub> we suggest here the next scheme of sensing. Along with standard H<sub>2</sub> interaction with tin dioxide surface the additional spillover effect takes place as NiO<sub>x</sub> clusters provide the conditions for H<sub>2</sub> molecules splitting [29]. In particular, it was shown in given work both theoretically and experimentally (AES studies) that no reaction between H<sub>2</sub> and the NiO(100) crystal after 50 min of exposure to the gas at  $1 \times 10^{-7}$  Torr and 350 °C, i.e. no any significant changes in the O/Ni AES ratio. Thus, it was concluded that the probability for the reaction



on a perfect NiO surface is very small ( $<10^{-3}$  per H<sub>2</sub> collision). However, the presence of large amount of the defects - oxygen vacancies – in the matrix of NiO<sub>x</sub> creates conditions for cleavage of H<sub>2</sub> molecules to atoms. The H<sub>2</sub> molecule is bridging two of the Ni atoms located around an O vacancy on NiO<sub>x</sub> surface and, as result, the H-H bond length increases to 0.87 Å, facilitating dissociation of the adsorbate. The similar result was obtained in [30] by a quantum chemical calculation, confirming that H<sub>2</sub> can be only *dissociatively* adsorbed on lattice defects on NiO<sub>x</sub>. In the result of hydrogen dissociation, the last one migrates to the SnO<sub>2</sub> surface and interacting with chemisorbed oxygen gives contribution to the change of the free electron concentration change in nanowire, stipulating further gas sensitivity growth.

#### 4. CONCLUSION

It was shown that *in situ* functionalization of SnO<sub>2</sub> nanowire with NiO<sub>x</sub> allows to well controlling the electrical characteristics of metal oxide nanowire and significantly improving its gas sensing performance. Developed chemoresistor has demonstrated extremely high sensitivity toward ppb level hydrogen and significantly improved selectivity toward hydrogen comparing with CO. Obtained results are explained with the model of NiO<sub>x</sub> cluster formation on the surface of SnO<sub>2</sub> nanowire.

#### ACKNOWLEDGEMENTS

Author would like to thank Dr. A. Kolmakov for the possibility to carry out this research in his Laboratory of the Surface Phenomena & Imaging of Nanostructures (Southern Illinois University at Carbondale (SIU), USA). Research work was supported via Seed Grant Program and Materials Technology Center Grant (both SIU).

#### REFERENCES

1. M. Law, H. Kind, B. Messer, F. Kim, and P.D. Yang, Photochemical Sensing of NO<sub>2</sub> with SnO<sub>2</sub> Nanoribbon Nanosensors at Room Temperature, *Angewandte Chemie-International Edition*, **41**, Issue 13, 2405–2408 (2002)
2. E. Comini, G. Faglia, G. Sberveglieri, Z.W. Pan, and Z.L. Wang, Stable and highly sensitive gas sensors based on semiconducting oxide nanobelts, *Applied Physics Letters*, **81**, Issue 10, 1869-1871 (2002)

3. C. Li, D.H. Zhang, X.L. Liu, S. Han, T. Tang, J. Han, and C.W. Zhou, In<sub>2</sub>O<sub>3</sub> nanowires as chemical sensors, *Applied Physics Letters*, **82**, Issue 10, 1613 (2003)
4. A. Kolmakov, Y.X. Zhang, G.S. Cheng, and M. Moskovits, Detection of CO and O<sub>2</sub> Using Tin Oxide Nanowire Sensors, *Advanced Materials*, **15**, 997 (2003)
5. A Maiti, J Rodriguez, M Law, P Kung, J McKinney, P Yang, SnO<sub>2</sub> Nanoribbons as NO<sub>2</sub> Sensors, *Nano Letters*, **3**, 1025-1028 (2003)
6. D. J. Zhang, C. Li, X. L. Liu, et al., Doping dependent NH<sub>3</sub> sensing of indium oxide nanowires, *Applied Physics Letters*, **83**, 1845 (2003)
7. Y. Zhang, A. Kolmakov, S. Chretien, et al., Control of catalytic reactions at the surface of a metal oxide nanowire by manipulating electron density inside it, *Nano Letters*, **4**, 403 (2004)
8. A. Kolmakov, D.O. Klenov, Y. Lilach, S. Stemmer, and M. Moskovits, Enhanced Gas Sensing by Individual SnO<sub>2</sub> Nanowires and Nanobelts Functionalized with Pd Catalyst Particles, *Nano Letters*, **5**, 667 (2005)
9. M. Curreli, C. Li, Y. Sun, B. Lei, M.A. Gundersen, M.E. Thompson, C. Zhou, Selective Functionalization of In<sub>2</sub>O<sub>3</sub> Nanowire Mat Devices for Bio-sensing Applications, *Journal of the American Chemical Society*, **127**, 6922–6923 (2005)
10. A. Alejandre, F. Medina, P. Salagre, A. Fabregat, J.E. Sueiras, Characterization and activity of copper and nickel catalysts for the oxidation of phenol aqueous solutions, *Applied Catalysis B-Environmental*, **18**, 307-315 (1998)
11. K. M. Dooley, S. Y. Chen, J. R. H. Ross, Stable Nickel-Containing Catalysts for the Oxidative Coupling of Methane, *J. Catal.*, **145**, 402-408 (1994).
12. R. X. Dingsheng Wang, Xun Wang and Yadong Li, NiO nanorings and their unexpected catalytic property for CO oxidation *Nanotechnology*, **17**, 979–983 (2006)
13. R. H. Kodama, S. A. Makhlof, A. E. Berkowitz, Finite Size Effects in Antiferromagnetic NiO Nanoparticles, *Physical Review Letters*, **79**, 1393 (1997)
14. T. M. H. Sato, S. Takata and T. Yamada, Transparent Conducting P-Type NiO<sub>x</sub> Thin Films Prepared by Magnetron Sputtering, *Thin Solid Films*, **236**, 27-31 (1993)
15. K. Yoshimura, T. Miki, and S. Tanemura, Nickel Oxide Electrochromic Thin Films Prepared by Reactive DC Magnetron Sputtering, *Japanese Journal of Applied Physics Part 1-Regular Papers Short Notes & Review Papers*, **34**, 2440 (1995)
16. T. P. A. Neubecker, T. Doll, W. Hansch and I. Eisele, Ozone-enhanced molecular beam

- deposition of nickel oxide (NiO) for sensor applications. *Thin Solid Films* **310**, 19-23 (1997)
17. J. H. I. Hotový, L. Spiess, R. Capkovic and S. Hascík, Preparation and characterization of NiO thin films for gas sensor applications, *Vacuum*, **58**, 300 (2000)
  18. M. Matsumiya, F. Qiu, W. Shin, N. Izu, N. Murayama, S. Kanzaki, Thin-film Li-doped NiO for thermoelectric hydrogen gas sensor, *Thin Solid Films*, **419**, 213 (2002)
  19. V. R. I. Hotovy, P. Siciliano, S. Capone, L. Spiess, Sensing characteristics of NiO thin films as NO<sub>2</sub> gas sensor, *Thin Solid Films*, **418**, 9 (2002)
  20. R. C. P. Hidalgo, A. Coelho, and D. Gouvêa, Surface segregation and consequent SO<sub>2</sub> sensor response in SnO<sub>2</sub>-NiO, *Chemistry of Materials*, **17**, 4149 (2005)
  21. D.F.Cox, T.B. Fryberger, S. Semancik. Oxygen vacancies and defect electronic states on the SnO<sub>2</sub> (110)-1x1 surface, *Physical Review B*, **38**, 2072-2083 (1988)
  22. C.G.Founstadt, R.H.Rediker, Electrical Properties of High-Quality Stannic Oxide Crystals, *J.Appl. Phys*, **42**, 2911-2918 (1971)
  23. Z.R. Dai, Z.W. Pan, and Z.L. Wang, Novel Nanostructures of Functional Oxides Synthesized by Thermal Evaporation, *Advanced Functional Materials*, **13**, 9, (2003)
  24. McCarthy and J.Welton, *Powder Diffraction*, **4**, 156 (1989)
  25. M. N. Rumyantseva, O. V. Safonova, M. N. Boulova, L. I. Ryabova, A. M. Gas'kov, *Russian Chemical Bulletin, International Edition*, Vol. 52, No. 6, pp. 1217—1238 (2003)
  26. B. Monnerat, L. Kiwi-Minsker, A. Renken, Mathematical modelling of the unsteady-state oxidation of nickel gauze catalysts, *Chemical Engineering Science*, **58**, 4911–4919 (2003)
  27. S. V.Kumari, M. Natarajan, V. K. Vaidyan, P. Koshy Surface oxidation of nickel thin films, *Journal of Materials Science Letters*, **11**, Iss.11, 761-762 (1992)
  28. A.M. Mebel, D.-Y. Hwang, Theoretical Study on the Reaction Mechanism of Nickel Atoms with Carbon Dioxide, *J. Phys. Chem. A*, **104** (49), pp 11622–11627, (2000)
  29. J.A. Rodrigez, J.C.Hanson, A. I. Frenkel J.Y.Kim, M.Perez, Experimental and Theoretical Studies on the Reaction of H<sub>2</sub> with NiO: Role of O Vacancies and Mechanism of Oxide Reduction, *J.Am. Chem. Soc.*, **124**, No.2, 346-354 (2002)
  30. P.K. de Bokx, F. Labohm, O.L.J. Gijzeman, G.A. Bootsma, J.W. Geus, The Interaction of Oxygen with Ni(100) and the Reduction of the Surface Oxide by Hydrogen, *Appl. Surf. Sci.*, **5**, 321—331, (1980)

